THE JOURNAL OF BIOLOGICAL CHEMISTRY VOL. 286, NO. 35, pp. 30526–30534, September 2, 2011

Substrate Specificity of Lymphoid-specific Tyrosine Phosphatase (Lyp) and Identification of Src Kinase-associated Protein of 55 kDa Homolog (SKAP-HOM) as a Lyp Substrate*

Received for publication, April 25, 2011, and in revised form, June 7, 2011 Published, JBC Papers in Press, June 30, 2011, DOI 10.1074/jbc.M111.254722

Xiao Yu[1,2], Ming Chen[1], Sheng Zhang, Zhi-Hong Yu, Jin-Peng Sun, Lina Wang, Sijiu Liu, Tsuyoshi Imasaki, Yuichiro Takagi, and Zhong-Yin Zhang[3]

From the Department of Biochemistry and Molecular Biology, Indiana University School of Medicine, Indianapolis, Indiana 46202

A missense single-nucleotide polymorphism in the gene encoding the lymphoid-specific tyrosine phosphatase (Lyp) has been identified as a causal factor in a wide spectrum of autoimmune diseases. Interestingly, the autoimmune-predisposing variant of Lyp appears to represent a gain-of-function mutation, implicating Lyp as an attractive target for the development of effective strategies for the treatment of many autoimmune disorders. Unfortunately, the precise biological functions of Lyp in signaling cascades and cellular physiology are poorly understood. Identification and characterization of Lyp substrates will help define the chain of molecular events coupling Lyp dysfunction to diseases. In the current study, we identified consensus sequence motifs for Lyp substrate recognition using an "inverse alanine scanning" combinatorial library approach. The intrinsic sequence specificity data led to the discovery and characterization of SKAP-HOM, a cytosolic adaptor protein required for proper activation of the immune system, as a *bona fide* Lyp substrate. To determine the molecular basis for Lyp substrate recognition, we solved crystal structures of Lyp in complex with the consensus peptide as well as the phosphopeptide derived from SKAP-HOM. Together with the biochemical data, the structures define the molecular determinants for Lyp substrate specificity and provide a solid foundation upon which novel therapeutics targeting Lyp can be developed for multiple autoimmune diseases.

Protein-tyrosine phosphorylation-mediated signal transduction is essential for a wide range of eukaryotic functions, including cell proliferation, differentiation, migration, apoptosis, and the immune responses (1). This signaling mechanism is often dysregulated in human diseases, due to aberrant activity of the enzymes involved in the regulation of protein tyrosine phosphorylation status (1, 2). Thus, a comprehensive understanding of the physiological roles of protein tyrosine phosphorylation and how this process is abrogated in the pathogenesis of human diseases must necessarily include characterization of protein-tyrosine phosphatases (PTPs),[4] in addition to protein-tyrosine kinases.

The lymphoid-specific tyrosine phosphatase (Lyp) has garnered tremendous interest due to the observation that a missense C1858T single nucleotide polymorphism in the gene (*PTPN22*) encoding Lyp is associated with multiple autoimmune disorders, including type I diabetes (3), rheumatoid arthritis (4, 5), Graves disease (6), and systemic lupus erythematosus (7). Lyp expression is restricted to human T cells, B cells, and macrophages (8). Lyp exerts an inhibitory effect on the proximal T cell receptor signaling pathways, probably through dephosphorylation of the Lck and ZAP-70 kinases (9–11). The C1858T single nucleotide polymorphism changes Arg^{620} into a Trp within the first Pro-rich region in the C terminus of Lyp, leading to loss of Lyp binding to the Src homology 3 domain of the Src C-terminal kinase (Csk) (3, 4). Importantly, the autoimmune-predisposing variant of Lyp appears to represent a gain-of-function mutation, leading to increased inhibition of T-cell signaling relative to the wild-type enzyme (12). Interestingly, a loss-of-function variant of *PTPN22* has been linked to reduced risk of systemic lupus erythematosus (13). Hence, Lyp is emerging as a potential target for therapeutic intervention of a broad spectrum of autoimmune disorders. Unfortunately, it remains unclear how an activating mutation in a negative regulator of T cell signaling gives rise to autoimmune diseases. Recent studies of *PTPN22* C1858T carriers also point to a role for Lyp in B cell signaling, indicating that a combination of disregulation of T cell, B cell, and possibly macrophage function by the Lyp/R620W mutant may contribute to autoimmunity (14–16).

Despite its involvement in many autoimmune diseases, the precise biological functions of Lyp in signaling cascades and cellular physiology are poorly understood (17). Key issues that need to be addressed include the full repertoire of Lyp substrates and the signaling cascades modulated by Lyp activity. It is likely that in addition to ZAP-70 and Src family tyrosine kinases, Lyp may act on other as yet unidentified substrates. Identification and characterization of novel Lyp substrates will help define the chain of molecular events coupling Lyp dysfunction to diseases. In the current study, we sought to determine

* This work was supported, in whole or in part, by National Institutes of Health Grants CA69202 and CA126937.

The atomic coordinates and structure factors (codes 3OLR and 3OMH) have been deposited in the Protein Data Bank, Research Collaboratory for Structural Bioinformatics, Rutgers University, New Brunswick, NJ (http://www.rcsb.org/).

[1] Both authors contributed equally to this work.

[2] Present address: Institute of Physiology, Shandong University School of Medicine, 44 Wenhua West Rd., Jinan, Shandong 250012, China.

[3] To whom correspondence should be addressed: Dept. of Biochemistry and Molecular Biology, Indiana University School of Medicine, 635 Barnhill Dr., Indianapolis, IN 46202. E-mail: zyzhang@iupui.edu.

[4] The abbreviations used are: PTP, protein-tyrosine phosphatase; Lyp, lymphoid-specific tyrosine phosphatase; r.m.s., root mean square.

Lyp substrate specificity using an "inverse alanine scanning" peptide library approach (18). The obtained consensus peptide corresponds to a stretch of amino acid sequence in the integrin-signaling adaptor SKAP-HOM (19, 20), which is a homolog of Src kinase-associated protein of 55 kDa (SKAP-55) (21). Biochemical and substrate-trapping studies support the notion that SKAP-HOM is a *bona fide* Lyp substrate. To determine the molecular basis for Lyp substrate recognition, we solved crystal structures of Lyp in complex with the consensus peptide as well as the phosphopeptide derived from SKAP-HOM. Together with the biochemical data, the structures define the molecular determinants for Lyp substrate specificity and provide a solid foundation upon which novel therapeutics targeting Lyp can be developed for multiple autoimmune disorders.

EXPERIMENTAL PROCEDURES

Materials—*p*-Nitrophenyl phosphate was purchased from Fluke. Glutathione-Sepharose 4B was from Amersham Biosciences. Rabbit Myc antibody was from Santa Cruz Biotechnology, Inc. (Santa Cruz, CA). Crystallization reagents were from Hampton Research. FLAG tag affinity beads, FLAG antibody, and all other reagents were obtained from Sigma.

Protein Expression and Purification—Expression and purification of the His-tagged Lyp catalytic domain (residues 1–294) were performed as described previously (22). For substrate trapping, the Lyp catalytic domain was subcloned into the pGEX-2T vector, and the GST-tagged Lyp protein was expressed in BL21 *Escherichia coli*. In general, 3 liters of GST-tagged Lyp transformed *E. coli* were cultured, induced by 0.6 mM isopropyl 1-thio-β-D-galactopyranoside, and pelleted by centrifugation at 5,000 rpm. The cell pellets were resuspended in 30 ml of a buffer containing 20 mM Tris, pH 7.5, 150 mM NaCl, 1 mM DTT, 2 mM EDTA, and 1 mM PMSF. The suspensions were twice frozen and thawed, and lysozymes were added at 1 mg/ml and incubated at room temperature for 30 min. Triton X-100 was subsequently added to a final concentration of 1% and incubated for another 20 min. The bacterial lysate was centrifuged at 12,000 rpm at 4 °C for 1 h, and the supernatant was collected and incubated with 1 ml of glutathione-Sepharose 4B. The suspension was mixed by end-over-end rotation for 1 h at 4 °C. The beads were pelleted at 1,000 rpm for 1 min, and the supernatant was discarded. The beads were washed four times for 10 min each at 4 °C each time. The bound GST-Lyp protein was finally eluted with a buffer containing 50 mM Tris, pH 8.0, and 10 mM reduced glutathione. The protein was further concentrated and stored at −20 °C. All Lyp mutants were generated by using the QuikChange site-directed mutagenesis kit from Stratagene.

Phosphatase Assay—Initial rate measurements for the Lyp-catalyzed *p*-nitrophenyl phosphate hydrolysis were carried out as described (22, 23). The Lyp-catalyzed hydrolysis of Tyr(P)-containing peptides was continuously monitored at 305 nm for the increase in tyrosine fluorescence with excitation at 280 nm (18). The reaction was conducted at 25 °C and pH 7.0 in 50 mM 3,3-dimethylglutarate buffer containing 1 mM EDTA, 1 mM DTT, with an ionic strength of 0.15 M adjusted by the addition of NaCl. When $[S] \ll K_m$, the Michaelis-Menten equation reduces to Equation 1.

$$v = \frac{k_{cat}}{K_m}[E][S] \quad \text{(Eq. 1)}$$

Under this condition, the reaction is first order with respect to [S]. At a given enzyme concentration, the observed apparent first order rate constant is equal to $(k_{cat}/K_m)[E]$. The substrate specificity constant k_{cat}/K_m value is calculated by dividing the apparent first order rate constant by the enzyme concentration. Fluorometric determinations were performed on a PerkinElmer Life Sciences 50B fluorometer. All reactions were initiated by the addition of Lyp to a final 3 nM concentration. The data were analyzed using a nonlinear least-squares regression program (KaleidaGraph, Synergy Software) and Igor Software (WaveMetrics, Lake Oswego, OR).

Peptide Synthesis and Characterization—The synthesis and characterization of the inverse alanine phosphopeptide library were described previously (18). The Lyp consensus peptides (Ac-YGEEpYDDLY-NH_2 and Ac-YGYEpYDDEY-NH_2) and the peptide ^{71}DGEEpYDDPF^{79} derived from SKAP-HOM were prepared using standard solid phase Fmoc (*N*-(9-fluorenyl)methoxycarbonyl) chemistry. The peptides were purified by HPLC using a Waters Breeze HPLC system equipped with a Waters Atlantis dC18 column (19 × 50 mm). The eluted phosphopeptides were lyophilized and redissolved in water. The phosphopeptide concentrations were determined by complete dephosphorylation using PTP1B and determination of the released inorganic phosphate. The sequence and the purity of the peptides were verified using an Agilent 1200 LC-MS system equipped with an Agilent Eclipse XDB-C18 analytical column (4.6 × 150 mm) and an Agilent 6130 Quadrupole MS detector.

BLAST Search—The Lyp consensus substrate peptide sequence YGEEYDDLY was subjected to BLAST analysis (on the NCBI, National Institutes of Health, Web site). The top scored proteins without a tyrosine at position 5 were manually excluded. The top five scored proteins were SKAP-HOM (^{71}DGEEYDDPF^{79}), phosphorylase kinase, α1 (^{628}YSEDYDDNY^{636}), B-cell scaffold protein with ankyrin repeats 1 (^{347}SEDQYDDLY^{355}), ADAM metallopeptidase with thrombospondin type 1 motif 13 (^{620}YGEEYGNLT^{628}), and lipoxygenase homology domain-containing protein 1 isoform 1 (^{1047}YGEEYGDTG^{1055}).

GST Pull-down—Five 10-cm dishes of RAW264.7 or five 150-cm^2 flasks of Jurkat T cells at 90% confluence were treated with 200 mM pervanadate for 5 min and then lysed in a buffer containing 20 mM HEPES pH 7.5, 100 mM NaCl, 0.5% Nonidet P-40, 5 mM iodoacetic acid, and a protease inhibitor mixture and rotated end-over-end at 4 °C for 1 h. After the addition of 10 mM DTT and 2 mM EDTA, the supernatant was recovered after centrifugation at 15,000 rpm for 15 min. The supernatant was left on ice for 10 min and then incubated with 5 μg of purified GST, GST-tagged wild-type Lyp catalytic domain, or C227S or D195A mutant Lyp for 1 h with end-over-end rotation at 4 °C. The GST-Lyp·substrate complex was then pulled down by incubating with 20 μl of GST-agarose beads and precipitated by centrifugation. The precipitated agarose beads were washed with a binding buffer (20 mM HEPES, pH 7.5, 1 mM DTT, 1 mM EDTA, and 100 mM NaCl) three times, and then an

equal volume of 2× SDS loading buffer was added and subjected to Western blot analysis.

Co-immunoprecipitation and Western Blotting—HEK293 cells were transiently co-transfected with FLAG-tagged SKAP-HOM together with Myc-tagged Lyp. The cells were stimulated with 50 ng/ml EGF for 5 min and then collected in lysis buffer (50 mM HEPES, 0.5% Nonidet P-40, 250 mM NaCl, 10% glycerol, 2 mM EDTA, 1 mM DTT, and protease inhibitor). The cell lysates were centrifuged at 15,000 rpm for 15 min after a 1-h end-over-end rotation at 4 °C. The complex of SKAP-HOM and Lyp was isolated by 20 μl of FLAG tag affinity beads. The isolated complex was subjected to electrophoresis, and the amount of Lyp bound to SKAP-HOM was measured by Myc antibodies.

Crystallization, Data Collection, and Structure Determination—The N-terminal His_6-tagged catalytically inactive Lyp/C227S (residues 1–294) mutant was crystallized with the phosphopeptides under conditions similar to those reported previously (22). The co-crystals of Lyp/C227S with the consensus or the SKAP-HOM peptide appeared after 3 days and grew to 0.1 × 0.2 × 0.2 mm after 5 days. X-ray diffraction data were collected up to 2.5 Å for Lyp/C227S in complex with the consensus peptide and 2.9 Å for Lyp/C227S in complex with the SKAP-HOM peptide at the APS 19BM beamline (Argonne, IL). The diffraction data were processed with HKL2000 (24). The crystals of Lyp/C227S with the consensus peptide belong to space group *P*1, whereas the crystals of Lyp/C227S with the SKAP-HOM peptide belong to space group $P2_1$, with four Lyp molecules in each asymmetric unit.

Initial phases of the Lyp/C227S-peptide complexes were determined by molecular replacement with the software Phaser from the CCP4 software package. A single chain of the Lyp catalytic domain from Protein Data Bank entry 2QCT was used as the initial search model, with water and I-C11 deleted from the coordinates. After one round of refinement with rigid body by Refmac in the CCP4 package, the coordinates and reflection data were transformed to CNS format, and further refinement was carried out in CNS (25). Composite omitted maps were built, and density modification was carried out to reduce the phase biases during further refinement. The final refined model has R_{work}/R_{free} at 0.162/0.210 for Lyp/C227S in complex with the consensus peptide **1** and 0.164/0.223 for Lyp/C227S in complex with the SKAP-HOM $Tyr(P)^{75}$ peptide. All data collection and refinement statistics are listed in Table 2. The final structures were deposited in the Protein Data Bank.

RESULTS AND DISCUSSION

Determination of Lyp Substrate Specificity—Although Lyp is associated with a wide range of autoimmune diseases, its physiological substrates and *in vivo* function remain poorly defined. Knowledge about the substrate specificity of Lyp will facilitate the identification of its physiological substrates and may ultimately assist in the design of Lyp-specific inhibitors. Previous kinetic and structural studies using synthetic Tyr(P)-containing peptides reveal that PTPs display a range of k_{cat}/K_m (substrate specificity constant) values (10^2 to 10^7 M^{-1} s^{-1}) for relatively short peptide substrates (26). In addition, the k_{cat}/K_m values for the peptides are orders of magnitude higher than that of Tyr(P) alone, suggesting that amino acids flanking the Tyr(P) also contribute to catalytic efficiency (27, 28). In fact, substrate recognition by PTPs requires the presence of amino acids on both the N- and C-terminal sides of Tyr(P) (29–31). However, because of the differences in sequence and size of the individual peptides examined, it is difficult to draw definitive conclusions regarding the structural requirements for PTP substrate recognition. A more systematic and thorough approach, such as the use of peptide libraries, is needed for the determination of substrate specificity for individual PTPs. Indeed, combinatorial peptide libraries have been useful in the determination of optimal amino acid sequence for PTP recognition (18, 32–38).

To identify novel Lyp substrates in an unbiased manner, we employed an "inverse alanine scanning" strategy (18) to profile the sequence specificity of Lyp. Briefly, each Ala residue in the parent peptide, Ac-AAAApYAAAA-NH_2, is separately and sequentially replaced by the 19 non-Ala amino acids to generate a library of 153 well defined phosphopeptides (Fig. 1). This method allows the acquisition of explicit kinetic data for all library members and enables the assessment of the contribution of individual amino acids to PTP substrate recognition based on the actual enzymatic activity of the PTP against its putative peptide substrates in solution. The Lyp-catalyzed dephosphorylation of each individual Tyr(P) peptide within the library was monitored by the increase in tyrosine fluorescence (18, 39) at pH 7.0 and 25 °C. The k_{cat}/K_m value, a measure of substrate specificity, was directly calculated from the reaction progress curve for each peptide (see "Experimental Procedures").

The results of the inverse alanine scanning of the entire peptide library for Lyp are shown in Fig. 1. The k_{cat}/K_m values for all 153 peptides ranged from 1.0×10^2 to 1.6×10^5 M^{-1} s^{-1}, covering over 3 orders of magnitude and varied significantly for different substitutions within a single position. The data indicate that incorporation of a Glu residue at position −1 furnishes the single most dramatic enhancement in substrate efficacy. To further substantiate this observation, we also re-synthesized the parent peptide Ac-AAAApYAAAA-NH_2, Ac-AAAEpYAAAA-NH_2, and Ac-AAAQpYAAAA-NH_2 and assayed them against Lyp under the same conditions. In full agreement with the library screening results, replacement of the Ala at the −1 position by Glu increased the k_{cat}/K_m value by 32-fold over the all-Ala parent peptide (5.0×10^3 M^{-1} s^{-1}), whereas the Gln substitution was only 6-fold better than the parent peptide (Table 1). A closer examination of the scanning data revealed a number of factors that control Lyp substrate specificity. Notable features of Lyp substrate specificity include the strong preference of acidic residues (Asp and Glu) at the −1, −2, +1, and +2 sites, although hydrophobic and aromatic residues could also be accommodated by Lyp at the −1 (Ile, Leu, Phe, and Tyr) and −2 (Trp and Tyr) positions. The +4 position is also an important determinant, which favors Trp and Tyr and, to a lesser extent, Glu and Gln as well. Lyp also shows a striking selectivity for Gly at the −3 position. A modest preference for Trp and Tyr is observed for position −4, and several structurally diverse residues, including Glu, Leu, Gln, Thr, and Val, can be tolerated at the +3-position. Finally, Lyp dislikes basic residues (Lys and Arg) at all positions.

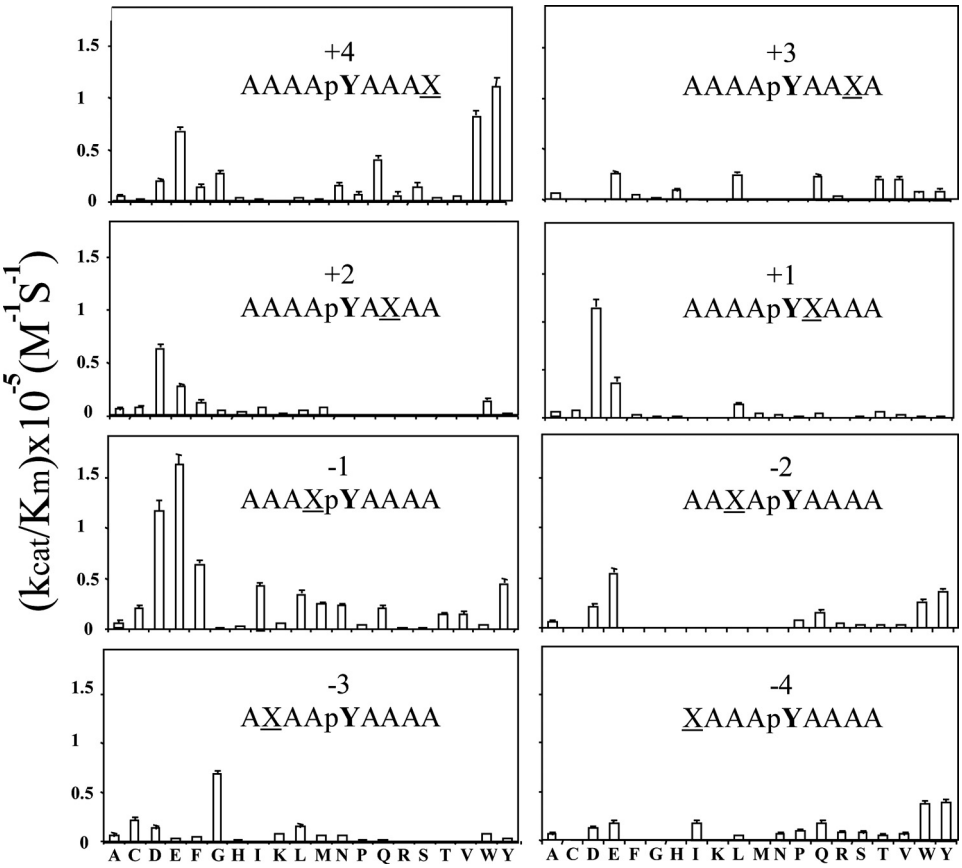

FIGURE 1. **Inverse alanine scanning of the whole library for Lyp.** The *k*cat/K_m values for the 153 peptides substituted from positions −4 to +4 are shown. All of the kinetic measurements were performed at pH 7.0 (50 mM 3,3-dimethylglutarate buffer, 1 mM EDTA, 1 mM DTT, ionic strength of 0.15 M adjusted by the addition of NaCl) and 25 °C. The data were the average of four independent measurements ± S.D. (*error bars*).

TABLE 1

k_{cat}/K_m values of Lyp toward Tyr(P)-containing peptides

All measurements were made at pH 7.0, 25 °C, and $I = 0.15$ M. The values were the average of three independent experiments, in duplicate. Errors reported are S.D. values.

Tyr(P) peptide	$k_{cat}/K_m \times 10^{-5}$
	$M^{-1}\,s^{-1}$
Ac-YGEEpYDDLY-NH_2 consensus peptide **1**	46 ± 0.5
Ac-DGEEpYDDPF-NH_2 SKAP-HOM Tyr^{75} peptide	40 ± 0.3
Ac-YGYEpYDDEY-NH_2 consensus peptide **2**	21 ± 0.1
Ac-ENDEpYTARE-NH_2 Lck Tyr^{394} peptide	6.2 ± 0.1
Ac-TEPQpYQPGE-NH_2 Lck Tyr^{505} peptide	0.6 ± 0.02
Ac-AAAApYAAAA-NH_2	0.05 ± 0.01
Ac-AAAEpYAAAA-NH_2	1.6 ± 0.1
Ac-AAAQpYAAAA-NH_2	0.3 ± 0.02

Based on the results from inverse alanine scanning of the 153-peptide library (Fig. 1), we synthesized two consensus peptides by combining the most preferred residue at each position. The consensus peptide **1** (Ac-YGEEpYDDLY-NH_2) and the consensus peptide **2** (Ac-YGYEpYDDEY-NH_2) represent the best peptide substrates ever reported for Lyp, exhibiting k_{cat}/K_m values of 4.6×10^6 M^{-1} s^{-1} and 2.1×10^6 M^{-1} s^{-1}, respectively, at pH 7.0 and 25 °C. The ~2-fold lower activity observed for consensus peptide **2** is consistent with the finding that Lyp has a higher preference for Glu than Tyr at the −2 position (Fig. 1). Previous studies showed that Lyp preferentially dephosphorylates Lck at $Tyr(P)^{397}$ in the activation loop over the autoinhibitory $Tyr(P)^{505}$ at its C terminus (11, 22). Consistent with this finding, the k_{cat}/K_m value for the Lck Tyr^{394} peptide (Ac-ENDEpYTARE-NH_2) is 10.3-fold higher than that of the Tyr^{505} peptide (Ac-TEPQpYQPGE-NH_2) (Table 1). Notably, the k_{cat}/K_m value for the Lck Tyr^{394} peptide is still 7.4-fold lower than that for the consensus peptide **1** (Table 1). The differences in the catalytic efficiency of Lyp toward these peptide substrates can be explained by the specificity data gained from inverse alanine scanning. Although the N-terminal amino acid sequence in the Lck Tyr^{394} peptide matches the specificity profile for Lyp, the Thr, Ala, and Arg at the C-terminal side of the Tyr(P) do not correspond to the most favored residues at the +1, +2, and +3 sites. The low activity of Lck Tyr^{505} peptide could be due to the fact that, with the exception of Gln^{-1} and Glu^{+4}, none of the other residues outperform Ala at the remaining positions (Table 1). Collectively, the kinetic analyses further validate the inverse alanine scanning approach for studying PTP substrate specificity (18), and the resulting specificity profile leads to the identification of consensus peptides that prove to be the best Lyp substrates known to date.

Sequence Specificity-based Substrate Identification for Lyp—Although PTPs share a common core catalytic domain with a conserved catalytic mechanism, in cellular environments, they carry out highly distinct, substrate-specific dephosphorylation events, which are essential for maintaining normal cellular processes. Knowledge about the substrate specificity of a given PTP can be used to facilitate the identification of its physiological substrates. Our current study establishes that Lyp exhibits

strong sequence specificity. To identify additional Lyp substrates, we launched a BLAST search using consensus peptide **1** (Table 1) as a query. The top hit corresponds to a sequence (^{71}DGEEYDDPF^{79}) within the human cytosolic adaptor molecule SKAP-HOM (19, 20), which is a homolog of Src kinase-associated protein of 55 kDa (SKAP-55) (21). Both SKAP-55 and SKAP-HOM are involved in the regulation of integrin activation and the related biological functions in immune cells (19). Whereas SKAP-55 is expressed solely in T lymphocytes (40), SKAP-HOM is more widely expressed in lymphohematopoietic cells (41–43). SKAP-55 and SKAP-HOM have the same molecular architecture, with an N-terminal dimerization domain, a central pleckstrin homology domain, and a C-terminal Src homology 3 domain. Interestingly, the tyrosine motif ^{71}DGEEYDDPF^{79} located in the linker between the dimerization domain and the pleckstrin homology domain in SKAP-HOM does not exist in SKAP-55.

To examine whether the phosphorylated tyrosine motif ^{71}DGEEYDDPF^{79} from SKAP-HOM could serve as a Lyp substrate, we synthesized the SKAP-HOM Tyr^{75} peptide (Ac-DGEEpYDDPF-NH_2) and assayed it against Lyp. Consistent with the prediction, the SKAP-HOM Tyr^{75} peptide is an excellent substrate for Lyp, with a k_{cat}/K_m value of 4.0×10^6 M^{-1} s^{-1}, comparable with that of the consensus peptide **1** (Table 1). Thus, the kinetic analysis suggests that SKAP-HOM Tyr^{75} is a potential cellular target of Lyp. To further establish that SKAP-HOM is a *bona fide* Lyp substrate, we decided to conduct substrate-trapping experiments in cells.

Two types of "substrate-trapping" mutants have been developed to identify PTP substrates. In the first, the active site Cys residue is replaced by a Ser (*e.g.* Lyp/C227S) (44), whereas in the second, the general acid Asp residue is substituted by an Ala (*e.g.* Lyp/D195A) (45). These mutant PTPs retain the ability to bind substrates but are either unable (the Cys to Ser mutant) or severely impaired (the Asp to Ala mutant) to carry out substrate dephosphorylation, allowing the capture of the PTP-substrate complex. In most cases, the Asp to Ala mutant displays a higher affinity toward substrates than the Cys to Ser mutant (45, 46). To investigate whether SKAP-HOM can serve as a substrate of Lyp in a cellular context, we first performed a GST pull-down experiment with pervanadate-treated (to increase and preserve tyrosine phosphorylation) RAW264.7 cell lysates with either GST alone, wild-type Lyp fused to GST (GST-Lyp), or the substrate-trapping fusion proteins GST-Lyp/C227S and GST-Lyp/D195A. Whereas no protein retained by GST or GST-Lyp was detectable, the GST-Lyp/C227S and GST-Lyp/D195A trapping mutants specifically bound SKAP-HOM (Fig. 2*A*). The failure to detect association of SKAP-HOM with wild-type Lyp indicates that the interaction between the Lyp trapping mutants and SKAP-HOM requires tyrosine phosphorylation, which is supported by the observation that the trapping mutant (especially GST-Lyp/D195A)-bound SKAP-HOM is tyrosine-phosphorylated (Fig. 2*A*). Because SKAP-55 lacks the SKAP-HOM Tyr(P)^{75} motif (the corresponding sequence in SKAP-55 is GQDSSDDNH), SKAP-55 is not expected to serve as a Lyp substrate. Indeed, Lyp trapping mutants GST-Lyp/C227S and GST-Lyp/D195A failed to bind SKAP-55 from Jurkat T cell lysates under similar pull-down conditions used for SKAP-HOM.[5] Finally, we analyzed whether Lyp forms a complex with SKAP-HOM inside the cell. Substrate trapping was performed in HEK293 cells expressing the FLAG-tagged SKAP-HOM together with the vector control pCDNA4, Myc-tagged Lyp, and Myc-tagged Lyp/D195A trapping mutant. Protein complexes were isolated from crude cell extracts using anti-FLAG antibodies to capture the FLAG-tagged SKAP-HOM, and the immunoprecipitates were examined for the presence of Myc-tagged Lyp by immunoblot analysis. As shown in Fig. 2*B*, SKAP-HOM readily coimmunoprecipitated with the substrate-trapping mutant Lyp/D195A. However, no complex formation was detected with wild-type Lyp or control transfectants lacking Lyp (Fig. 2*B*). Collectively, the results demonstrate specific interaction between the Lyp substrate-trapping mutant and SKAP-HOM, further confirming SKAP-HOM as a *bona fide* Lyp substrate.

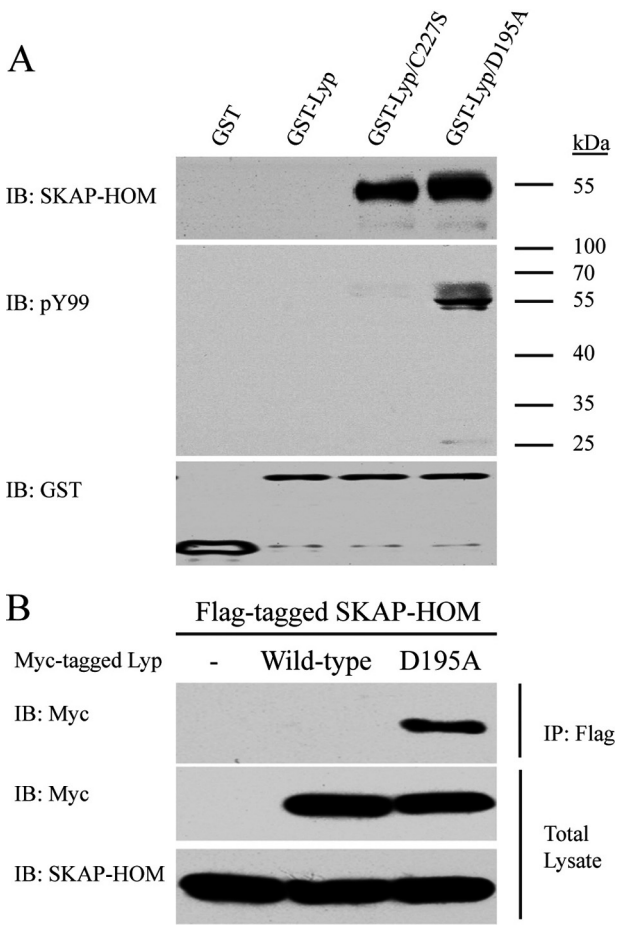

FIGURE 2. **SKAP-HOM is a *bona fide* substrate of Lyp.** *A*, endogenous SKAP-HOM in RAW264.7 cells could be pulled down by GST-Lyp/C227S or GST-Lyp/D195A substrate-trapping mutants. *B*, confirmation of the Lyp/SKAP-HOM interaction in HEK293 cells expressing both FLAG-tagged SKAP-HOM and Myc-tagged Lyp. SKAP-HOM was immunoprecipitated by FLAG beads, and its association with the Lyp/D195A trapping mutant was detected by anti-Myc antibody. Data are representative of three independent experiments. *IB*, immunoblot; *IP*, immunoprecipitation.

SKAP-HOM is a substrate for the Src family protein-tyrosine kinase Fyn and is involved in regulating leukocyte adhesion (19,

[5] X. Yu, M. Chen, S. Zhang, Z.-H. Yu, J.-P. Sun, L. Wang, S. Liu, T. Imasaki, Y. Takagi, and Z.-Y. Zhang, unpublished observations.

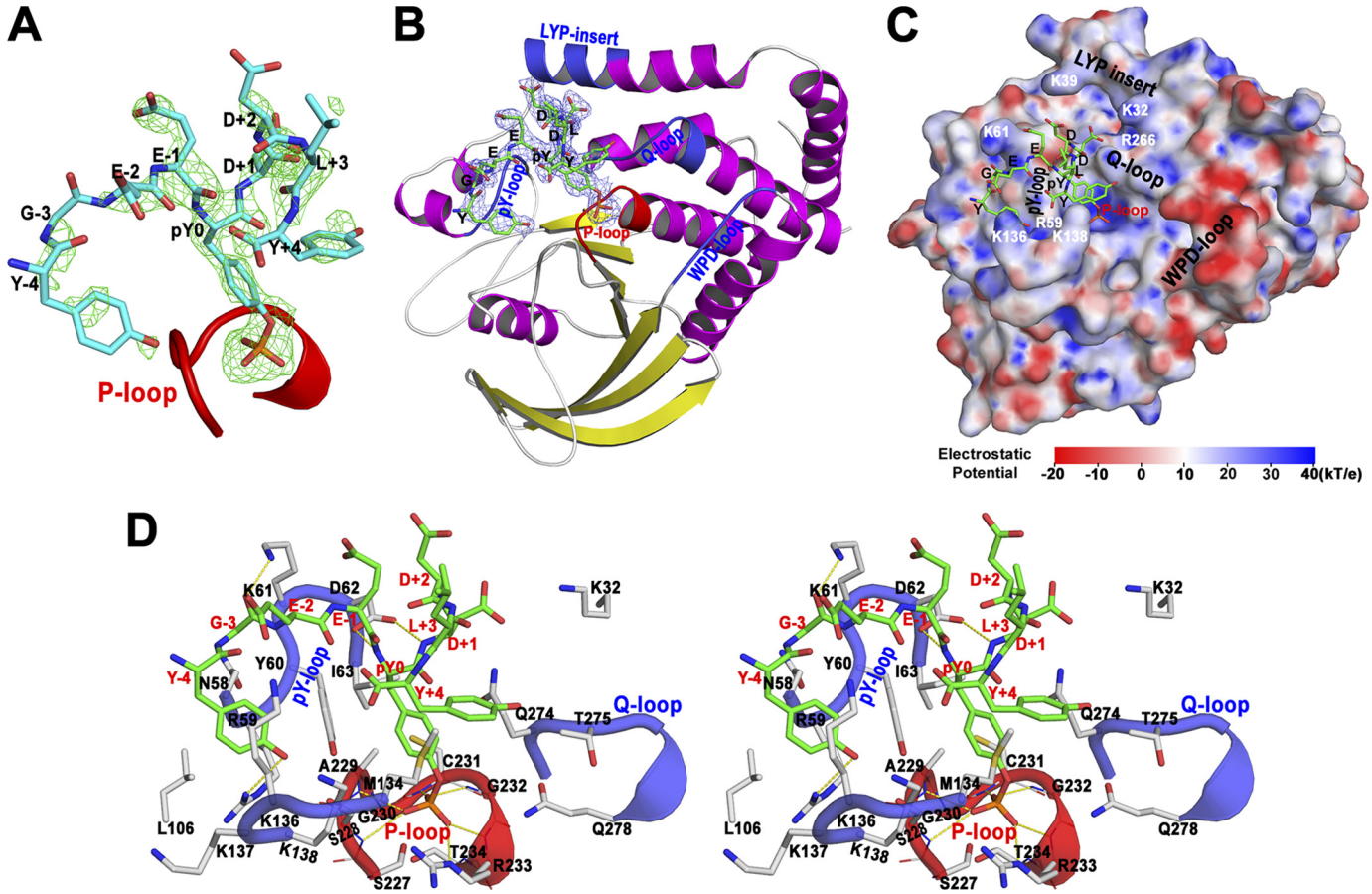

FIGURE 3. **Structure of Lyp in complex with the consensus peptide 1.** *A*, $F_o - F_c$ omit map (contoured at 3.0 σ) around the consensus peptide **1** (YGEEpY-DDLY). The peptide was omitted when calculating the $F_o - F_c$ map. *B*, *ribbon diagram* of the Lyp/C227S-peptide **1** structure. The P-loop is *highlighted* in *red*, and the WPD-loop, Q-loop, Lyp insert, and Tyr(P) loop (*pY-loop*) are *highlighted* in *blue*. The consensus peptide **1** is shown in a *stick representation* with its $2F_o - F_c$, electron density map contoured at 1.0 σ. *C*, the surface representation of the Lyp/C227S-peptide **1** structure. The protein is shown in a *surface representation* and *colored* by the electrostatic potential. The basic residues constituting the broad electropositive surface near the active site are *labeled*. *D*, stereo view showing detailed interactions of the consensus peptide **1** with Lyp/C227S. The consensus peptide **1** (*green carbon*) and interacting residues in Lyp/C227S (*gray carbon*) within 5 Å of the peptide are represented in a *stick model*; P-loop is depicted in a *red schematic*; and the Q-loop, Tyr(P) loop, and another neighboring loop are represented in *blue*. *Yellow dashed lines* represent direct hydrogen bond interactions.

47, 48). In SKAP-HOM-deficient mice, B cell receptor-mediated proliferation is strongly attenuated, and adhesion of activated B cells to fibronectin as well as to ICAM-1 is strongly reduced (48). In addition, the loss of SKAP-HOM also results in a less severe clinical course of experimental autoimmune encephalomyelitis following immunization of mice with the encephalitogenic peptide of myelin oligodendrocyte glycoprotein. Thus, it appears that SKAP-HOM is required for proper activation of the immune system, probably by regulating the cross-talk between immunoreceptors and integrins in B cells. Future studies will be required to delineate the role of Lyp-mediated SKAP-HOM dephosphorylation in B cell signaling and behaviors and to furnish new insight into how deregulation of Lyp activity contributes to autoimmune diseases.

Molecular Basis of Lyp Substrate Recognition—To determine the molecular basis of Lyp substrate recognition, we solved the crystal structures of the catalytically inactive mutant Lyp/C227S complexed with consensus peptide **1** and the SKAP-HOM Tyr(P)[75] peptide at 2.5 and 2.9 Å resolution, respectively (Figs. 3 and 4). Data collection and structure refinement statistics are summarized in Table 2. The final models for both structures include Lyp residues 1–294. Although the two structures belong to different space groups, both of them contain four monomers in an asymmetric unit with a 1:1 binding (Lyp/C227S to phosphopeptide) stoichiometry within each monomer. Initial $F_o - F_c$ omit maps displayed good density for Tyr(P) and its four neighboring residues (−2, −1, +1, and +2) at the Lyp catalytic active site (Figs. 3*A* and 4*A*). After iterative model building and refinement, the rest of the peptide was modeled into the well defined $2F_o - F_c$ electron density (Figs. 3*B* and 4*B*). The overall structures of Lyp/C227S in the two complexes are almost identical to each other (Cα r.m.s. deviation 0.45 Å) and very similar to the previously determined Lyp structure in complex with a small molecule inhibitor (22) (Cα r.m.s. deviation 1.1 Å). Unlike PTP1B, where peptide substrate binding induces the closure of the WPD-loop (encompassing residues 191–199 in Lyp) (29, 31), the WPD-loop in both of the Lyp/C227S-peptide complexes exists in the open conformation.

The peptide backbones of the bound Tyr(P) peptides adopt an "M"-shaped overall conformation, with the pentapeptide core EEpYDD assuming the central "V" shape, which is stabilized by two hydrogen bonds formed by the side chain of Asp^{62} with the main chain amides of Tyr(P) and Asp^{+1}. From the N to C terminus, the peptides interact with several surface loops in

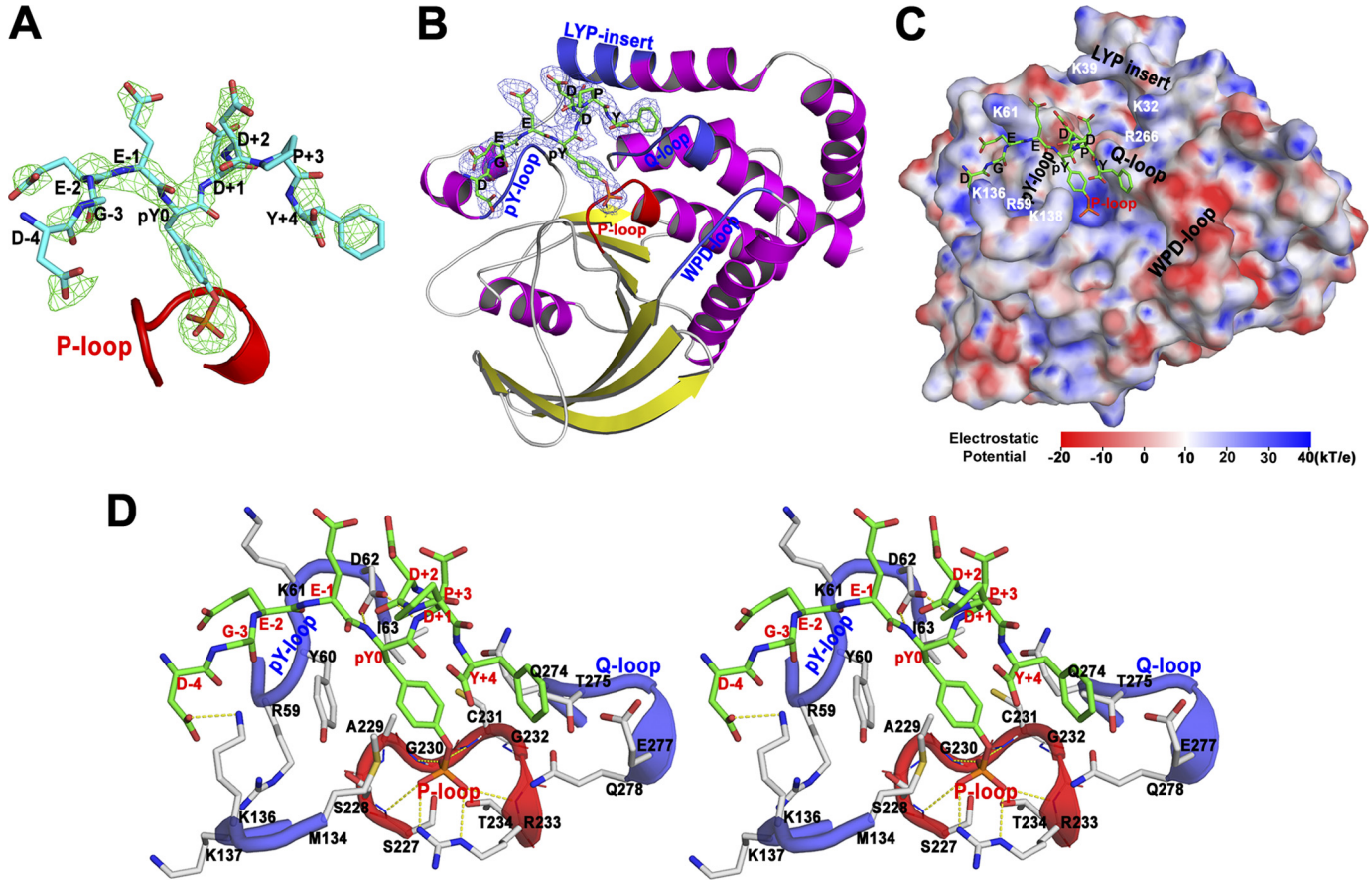

FIGURE 4. **Crystal structure of Lyp in complex with the SKAP-HOM Tyr(P)^{75} peptide.** *A*, $F_o - F_c$ omit map (contoured at 3.0 σ) around the SKAP-HOM Tyr(P)^{75} peptide (DGEEpYDDPF). The peptide was omitted when calculating the $F_o - F_c$ map. *B*, *ribbon diagram* of the Lyp/C227S·SKAP-HOM Tyr(P)^{75} peptide structure. The P-loop is *highlighted* in *red*; the WPD-loop, Q-loop, Lyp insert, and Tyr(P) loop are highlighted in *blue*. The SKAP-HOM Tyr(P)^{75} peptide is shown in a *stick representation* with its $2F_o - F_c$ electron density map contoured at 1.0 σ. *C*, *surface representation* of Lyp/C227S·SKAP-HOM Tyr(P)^{75} peptide structure. The protein is shown in a *surface representation* and *colored* by the electrostatic potential. The basic residues constituting the broad electropositive surface near the active site are *labeled*. *D*, stereo view showing detailed interactions of the SKAP-HOM Tyr(P)^{75} peptide with Lyp/C227S. The SKAP-HOM Tyr(P)^{75} peptide (green carbon) and interacting residues in Lyp/C227S (*gray carbon*) within 5 Å of the peptide are represented in a *stick model*; the P-loop is depicted in a *red schematic*; and the Q-loop, Tyr(P) loop (*pY-loop*), and another neighboring loop are represented in *blue*. *Yellow dashed lines* represent direct hydrogen bond interactions.

Lyp (Figs. 3*B* and 4*B*), including the Tyr(P) recognition loop (residues 58–63), the Lyp-specific insert (residues 35–42), the phosphate-binding loop (P-loop, residues 226–235), and the Q-loop (residues 269–278). In particular, the Lyp substrate-binding site contains a cluster of polar residues from the P-loop and additional basic residues (Lys^{32}, Lys^{39}, Arg^{59}, Lys^{61}, Lys^{136}, Lys^{138}, and Arg^{266}) that provides a complementary positive surface to the highly electronegative pentapeptide core EEpYDD (Figs. 3*C* and 4*C*). This electrostatic complementarity dictates the overall preference of Lyp for acidic residues at the −2, −1, +1, and +2 positions.

In the structure of Lyp/C227S-consensus peptide **1** complex, a rich network of interactions is responsible for the precise positioning of the peptide substrate (Fig. 3*D*). The central Tyr(P) is primarily anchored by six hydrogen bonds with backbone amides of Ser^{228}, Ala^{229}, Cys^{231}, Gly^{232}, and Arg^{233}, as well as the ϵ-N of Arg^{233} in the P-loop. Together with Van der Waals contacts with the side chains of Tyr^{60}, Ile^{63}, Ala^{229}, and aliphatic carbons of Gln^{274}, the Tyr(P) is tightly fixed at the active site pocket. As mentioned above, two hydrogen bonds, formed by the side chain of Asp^{62} with the backbone amides of Tyr(P) and Asp^{+1}, define the "V"-shaped binding conformation of the EEpYDD motif, allowing the N-terminal portion of the peptide to spread along the Lyp-specific insert and Tyr(P) recognition loop, whereas the C-terminal portion extends around the P-loop, Lyp-specific insert, and Q-loop. Specifically, Glu^{-1} engages in electrostatic interaction with Lys^{61} and also makes Van der Waals contacts with Lys^{61} and Asp^{62}. Glu^{-2} interacts electrostatically with Lys^{61}, Lys^{136}, and Lys^{138}, and its aliphatic carbons are involved in hydrophobic interactions with Tyr^{60}. These structural observations are consistent with the preference of Lyp for acidic residues and its plasticity for hydrophobic residues at −1 and −2 positions. The backbone amide of Gly^{-3} forms a hydrogen bond with Lys^{61}. Tyr^{-4} forms a hydrogen bond with Arg^{59} and makes hydrophobic interactions with Leu^{106}, Tyr^{60}, and the aliphatic carbons of Arg^{59} and Lys^{138}, which agrees well with the observed preference for Tyr and Trp at the −4 position. At the C-terminal side of Tyr(P), electrostatic interactions occur between Asp^{+1} and Lys^{32}, Gln^{274}, and Arg^{266}, and Asp^{+2} only makes long range polar interactions with Lys^{32} and Lys^{39}. These electrostatic interactions probably explain the overwhelming preference for acid residues at both the +1 and +2 positions. The following Leu^{+3} has no obvious interaction with Lyp, which is in accord with the fact that sev-

TABLE 2
Crystallographic data and refinement statistics

Parameters	Values	
	Lyp/C227S-consensus peptide 1	Lyp/C227S·SKAP-HOM Tyr(P)-75 peptide
Data collection		
Space group	P_1	$P2_1$
Cell dimensions		
a (Å)	45.9	115.2
b (Å)	62.8	46.7
c (Å)	117.5	121.5
α (degrees)	99.1	90.0
β (degrees)	96.5	101.4
γ (degrees)	105.1	90.0
Resolution (Å)	80-2.5 (2.6-2.5)[a]	80-2.9 (3.0-2.9)[a]
Unique observations	41,703	27,202
Completeness (%)	97.6 (95.7)[a]	94.6 (84.8)[a]
Redundancy	2.2 (2.1)[a]	3.2 (2.4)[a]
$\langle I \rangle / \langle \sigma \rangle$	14.0 (2.2)[a]	7.3 (1.9)[a]
R_{merge}	0.087 (0.371)[a]	0.091 (0.433)[a]
Structure refinement		
Resolution (Å)	80-2.5	80-2.9
No. of reflections used for R_{work} /R_{free}	34,551/3,486	23,389/2,277
R_{work}/R_{free} [b] (%)	0.162/0.210	0.164/0.223
Average *B*-factor		
Protein	30.6	32.9
Peptide	41.6	35.9
r.m.s. deviation ideal bonds (Å)	0.006	0.007
r.m.s. deviation ideal angles (deg)	1.22	1.31
Ramachandran plot (%)		
Most favored	86.2	84.0
Allowed	12.3	13.4
Generously allowed	1.4	2.0
Disallowed	0	0.6

[a] The values in parentheses correspond to the highest resolution shell.
[b] R_{free} was calculated based on a random 8.2% (for Lyp/C227S-consensus peptide **1**) or 7.9% (for Lyp/C227S·SKAP-HOM Tyr(P)^{75} peptide)of all reflections.

eral structurally diverse residues can be tolerated at the +3 position. Tyr^{+4} mainly makes hydrophobic interactions with Met^{134} and aliphatic carbons of Gln^{274} and Thr^{275}, in agreement with observed preference for large hydrophobic residues (Trp and Tyr) at the +4 position.

The structure of Lyp/C227S·SKAP-HOM Tyr(P)^{75} peptide reveals that the EEpYDD motif takes up a conformation similar to that observed in the Lyp/C227S-consensus peptide **1** structure (Fig. 4). Consequently, the interactions between Lyp and substrate residues from −2 to +2 are conserved for both consensus peptide **1** and the SKAP-HOM Tyr(P)^{75} peptide. Different from consensus peptide **1**, the SKAP-HOM Tyr(P)^{75} peptide assumes a more extended conformation at both termini. The −4 position is occupied by an Asp in the SKAP-HOM Tyr(P)^{75} peptide, which is displaced from the position taken by Tyr^{-4} in consensus peptide **1** and is surrounded by Arg^{59}, Lys^{136}, Lys^{137}, and Lys^{138}. The flexibility of a Gly at the −3 position may facilitate this displacement to optimize Lyp-peptide interactions based on the hydrophobic or acidic properties of the −4 residue. At the C terminus, no obvious interaction exist between Pro^{+3} and Lyp. However, the special backbone torsion angles of Pro^{+3} orient Phe^{+4} closer to the Q-loop in comparison with Tyr^{+4} in consensus peptide **1**, probably resulting in stronger hydrophobic interactions between Phe^{+4} and Met^{134} as well as side chains of Gln^{274}, Thr^{275}, and Glu^{277} in the Q-loop. Collectively, the observed interactions between Lyp and the SKAP-HOM Tyr(P)^{75} peptide agree with the excellent activity of Lyp toward the SKAP-HOM peptide and support the hypothesis that SKAP-HOM is a cellular substrate of Lyp.

In summary, consensus sequence motifs for Lyp substrate recognition were identified using an "inverse alanine scanning" combinatorial peptide library approach. The intrinsic sequence specificity data led to the discovery of SKAP-HOM as a potential cellular target of Lyp. Further biochemical and substrate-trapping experiments confirmed SKAP-HOM as a *bona fide* Lyp substrate. SKAP-HOM is a cytosolic adaptor protein required for proper activation of the immune system, probably by regulating the cross-talk between immunoreceptors and integrins in B cells. Further investigation of the functional consequence of Lyp-mediated SKAP-HOM dephosphorylation will shed new light on the molecular events coupling Lyp dysfunction to autoimmune diseases. The successful identification of SKAP-HOM as a Lyp substrate from peptide specificity profile suggests that the intrinsic sequence specificity of Lyp is a major determinant of the enzyme's *in vivo* substrate selectivity. Structural analysis of Lyp/C227S bound with consensus peptide **1** and SKAP-HOM Tyr(P)^{75} peptide revealed unique molecular determinants supporting the observed Lyp substrate specificity. The defined structural features of Lyp interactions with highly efficient peptide substrates could be exploited for the design of novel inhibitors of this enzyme for both mechanistic studies of Lyp signaling and therapeutic development.

REFERENCES

1. Hunter, T. (2009) *Curr. Opin. Cell Biol.* **21,** 140–146
2. Tonks, N. K. (2006) *Nat. Rev. Mol. Cell Biol.* **7,** 833–846
3. Bottini, N., Musumeci, L., Alonso, A., Rahmouni, S., Nika, K., Rostamkhani, M., MacMurray, J., Meloni, G. F., Lucarelli, P., Pellecchia, M., Eisenbarth, G. S., Comings, D., and Mustelin, T. (2004) *Nat. Genet.* **36,** 337–338
4. Begovich, A. B., Carlton, V. E., Honigberg, L. A., Schrodi, S. J., Chokkalingam, A. P., Alexander, H. C., Ardlie, K. G., Huang, Q., Smith, A. M., Spoerke, J. M., Conn, M. T., Chang, M., Chang, S. Y., Saiki, R. K., Catanese, J. J., Leong, D. U., Garcia, V. E., McAllister, L. B., Jeffery, D. A., Lee, A. T.,

Batliwalla, F., Remmers, E., Criswell, L. A., Seldin, M. F., Kastner, D. L., Amos, C. I., Sninsky, J. J., and Gregersen, P. K. (2004) *Am. J. Hum. Genet.* **75,** 330–337
5. Carlton, V. E., Hu, X., Chokkalingam, A. P., Schrodi, S. J., Brandon, R., Alexander, H. C., Chang, M., Catanese, J. J., Leong, D. U., Ardlie, K. G., Kastner, D. L., Seldin, M. F., Criswell, L. A., Gregersen, P. K., Beasley, E., Thomson, G., Amos, C. I., and Begovich, A. B. (2005) *Am. J. Hum. Genet.* **77,** 567–581
6. Smyth, D., Cooper, J. D., Collins, J. E., Heward, J. M., Franklyn, J. A., Howson, J. M., Vella, A., Nutland, S., Rance, H. E., Maier, L., Barratt, B. J., Guja, C., Ionescu-Tîrgoviste, C., Savage, D. A., Dunger, D. B., Widmer, B., Strachan, D. P., Ring, S. M., Walker, N., Clayton, D. G., Twells, R. C., Gough, S. C., and Todd, J. A. (2004) *Diabetes* **53,** 3020–3023
7. Kyogoku, C., Langefeld, C. D., Ortmann, W. A., Lee, A., Selby, S., Carlton, V. E., Chang, M., Ramos, P., Baechler, E. C., Batliwalla, F. M., Novitzke, J., Williams, A. H., Gillett, C., Rodine, P., Graham, R. R., Ardlie, K. G., Gaffney, P. M., Moser, K. L., Petri, M., Begovich, A. B., Gregersen, P. K., and Behrens, T. W. (2004) *Am. J. Hum. Genet.* **75,** 504–507
8. Cohen, S., Dadi, H., Shaoul, E., Sharfe, N., and Roifman, C. M. (1999) *Blood* **93,** 2013–2024
9. Gjörloff-Wingren, A., Saxena, M., Williams, S., Hammi, D., and Mustelin, T. (1999) *Eur. J. Immunol.* **29,** 3845–3854
10. Cloutier, J. F., and Veillette, A. (1999) *J. Exp. Med.* **189,** 111–121
11. Wu, J., Katrekar, A., Honigberg, L. A., Smith, A. M., Conn, M. T., Tang, J., Jeffery, D., Mortara, K., Sampang, J., Williams, S. R., Buggy, J., and Clark, J. M. (2006) *J. Biol. Chem.* **281,** 11002–11010
12. Vang, T., Congia, M., Macis, M. D., Musumeci, L., Orrú, V., Zavattari, P., Nika, K., Tautz, L., Taskén, K., Cucca, F., Mustelin, T., and Bottini, N. (2005) *Nat. Genet.* **37,** 1317–1319
13. Orrú, V., Tsai, S. J., Rueda, B., Fiorillo, E., Stanford, S. M., Dasgupta, J., Hartiala, J., Zhao, L., Ortego-Centeno, N., D'Alfonso, S., Arnett, F. C., Wu, H., Gonzalez-Gay, M. A., Tsao, B. P., Pons-Estel, B., Alarcon-Riquelme, M. E., He, Y., Zhang, Z. Y., Allayee, H., Chen, X. S., Martin, J., and Bottini, N. (2009) *Hum. Mol. Genet.* **18,** 569–579
14. Rieck, M., Arechiga, A., Onengut-Gumuscu, S., Greenbaum, C., Concannon, P., and Buckner, J. H. (2007) *J. Immunol.* **179,** 4704–4710
15. Arechiga, A. F., Habib, T., He, Y., Zhang, X., Zhang, Z. Y., Funk, A., and Buckner, J. H. (2009) *J. Immunol.* **182,** 3343–3347
16. Stanford, S. M., Mustelin, T. M., and Bottini, N. (2010) *Semin. Immunopathol.* **32,** 127–136
17. Siminovitch, K. A. (2004) *Nat. Genet.* **36,** 1248–1249
18. Vetter, S. W., Keng, Y. F., Lawrence, D. S., and Zhang, Z. Y. (2000) *J. Biol. Chem.* **275,** 2265–2268
19. Wang, H., and Rudd, C. E. (2008) *Trends Cell Biol.* **18,** 486–493
20. Swanson, K. D., Tang, Y., Ceccarelli, D. F., Poy, F., Sliwa, J. P., Neel, B. G., and Eck, M. J. (2008) *Mol. Cell* **32,** 564–575
21. Wang, H., Moon, E. Y., Azouz, A., Wu, X., Smith, A., Schneider, H., Hogg, N., and Rudd, C. E. (2003) *Nat. Immunol.* **4,** 366–374
22. Yu, X., Sun, J. P., He, Y., Guo, X., Liu, S., Zhou, B., Hudmon, A., and Zhang, Z. Y. (2007) *Proc. Natl. Acad. Sci. U.S.A.* **104,** 19767–19772
23. Sun, J. P., Fedorov, A. A., Lee, S. Y., Guo, X. L., Shen, K., Lawrence, D. S., Almo, S. C., and Zhang, Z. Y. (2003) *J. Biol. Chem.* **278,** 12406–12414
24. Otwinowski, Z., and Minor, W. (1997) *Methods Enzymol.* **276,** 307–326
25. Brünger, A. T., Adams, P. D., Clore, G. M., DeLano, W. L., Gros, P., Grosse-Kunstleve, R. W., Jiang, J. S., Kuszewski, J., Nilges, M., Pannu, N. S., Read, R. J., Rice, L. M., Simonson, T., and Warren, G. L. (1998) *Acta Crystallogr. D* **54,** 905–921
26. Zhang, Z. Y. (2002) *Annu. Rev. Pharmacol. Toxicol.* **42,** 209–234
27. Zhang, Z. Y., Thieme-Sefler, A. M., Maclean, D., McNamara, D. J., Dobrusin, E. M., Sawyer, T. K., and Dixon, J. E. (1993) *Proc. Natl. Acad. Sci. U.S.A.* **90,** 4446–4450
28. Zhang, Z. Y., Maclean, D., McNamara, D. J., Sawyer, T. K., and Dixon, J. E. (1994) *Biochemistry* **33,** 2285–2290
29. Jia, Z., Barford, D., Flint, A. J., and Tonks, N. K. (1995) *Science* **268,** 1754–1758
30. Yang, J., Cheng, Z., Niu, T., Liang, X., Zhao, Z. J., and Zhou, G. W. (2000) *J. Biol. Chem.* **275,** 4066–4071
31. Sarmiento, M., Puius, Y. A., Vetter, S. W., Keng, Y. F., Wu, L., Zhao, Y., Lawrence, D. S., Almo, S. C., and Zhang, Z. Y. (2000) *Biochemistry* **39,** 8171–8179
32. Cheung, Y. W., Abell, C., and Balasubramanian, S. (1997) *J. Am. Chem. Soc.* **119,** 9568–9569
33. Pellegrini, M. C., Liang, H., Mandiyan, S., Wang, K., Yuryev, A., Vlattas, I., Sytwu, T., Li, Y. C., and Wennogle, L. P. (1998) *Biochemistry* **37,** 15598–15606
34. Huyer, G., Kelly, J., Moffat, J., Zamboni, R., Jia, Z., Gresser, M. J., and Ramachandran, C. (1998) *Anal. Biochem.* **258,** 19–30
35. Wälchli, S., Espanel, X., Harrenga, A., Rossi, M., Cesareni, G., and Hooft van Huijsduijnen, R. (2004) *J. Biol. Chem.* **279,** 311–318
36. Espanel, X., and Hooft van Huijsduijnen, R. (2005) *Methods* **35,** 64–72
37. Sun, H., Tan, L. P., Gao, L., and Yao, S. Q. (2009) *Chem. Commun.* **6,** 677–679
38. Ren, L., Chen, X., Luechapanichkul, R., Selner, N. G., Meyer, T. M., Wavreille, A. S., Chan, R., Iorio, C., Zhou, X., Neel, B. G., and Pei, D. (2011) *Biochemistry* **50,** 2339–2356
39. Zhang, Z. Y., Maclean, D., Thieme-Sefler, A. M., Roeske, R. W., and Dixon, J. E. (1993) *Anal. Biochem.* **211,** 7–15
40. Marie-Cardine, A., Bruyns, E., Eckerskorn, C., Kirchgessner, H., Meuer, S. C., and Schraven, B. (1997) *J. Biol. Chem.* **272,** 16077–16080
41. Curtis, D. J., Jane, S. M., Hilton, D. J., Dougherty, L., Bodine, D. M., and Begley, C. G. (2000) *Exp. Hematol.* **28,** 1250–1259
42. Kouroku, Y., Soyama, A., Fujita, E., Urase, K., Tsukahara, T., and Momoi, T. (1998) *Biochem. Biophys. Res. Commun.* **252,** 738–742
43. Marie-Cardine, A., Verhagen, A. M., Eckerskorn, C., and Schraven, B. (1998) *FEBS Lett.* **435,** 55–60
44. Bliska, J. B., Clemens, J. C., Dixon, J. E., and Falkow, S. (1992) *J. Exp. Med.* **176,** 1625–1630
45. Flint, A. J., Tiganis, T., Barford, D., and Tonks, N. K. (1997) *Proc. Natl. Acad. Sci. U.S.A.* **94,** 1680–1685
46. Xie, L., Zhang, Y. L., and Zhang, Z. Y. (2002) *Biochemistry* **41,** 4032–4039
47. Black, D. S., Marie-Cardine, A., Schraven, B., and Bliska, J. B. (2000) *Cell Microbiol.* **2,** 401–414
48. Togni, M., Swanson, K. D., Reimann, S., Kliche, S., Pearce, A. C., Simeoni, L., Reinhold, D., Wienands, J., Neel, B. G., Schraven, B., and Gerber, A. (2005) *Mol. Cell. Biol.* **25,** 8052–8063